

ORBITAL ANGULAR MOMENTUM PARTON DISTRIBUTIONS IN QUARK MODELS

SERGIO SCOPETTA AND VICENTE VENTO

*Departament de Física Teòrica, Universitat de València, 46100 Burjassot
(València), Spain*

E-mail: sergio.scopetta@uv.es, vicente.vento@uv.es

At the low energy, *hadronic*, scale we calculate Orbital Angular Momentum (OAM) twist-two parton distributions for the relativistic MIT bag model and for non-relativistic quark models. We reach the scale of the data by leading order evolution in perturbative QCD. We confirm that the contribution of quarks and gluons OAM to the nucleon spin grows with Q^2 , and it can be relevant at the experimental scale, even if it is negligible at the hadronic scale, irrespective of the model used. The sign and shape of the quark OAM distribution at high Q^2 may depend strongly on the relative size of the OAM and spin distributions at the hadronic scale. Sizeable quark OAM distributions at the hadronic scale, as proposed by several authors, can produce the dominant contribution to the nucleon spin at high Q^2 .

1 Introduction

Understanding how the partons carry the angular momentum in the nucleon has become a main effort of present day physics. The quark spin contribution $\Delta\Sigma$ is well defined in QCD¹, thus measurable; with respect to the gluon spin contribution Δg , the experimental² and theoretical³ situation has been discussed at the Conference. Our knowledge of the quark, L_q and gluon, L_g , Orbital Angular Momentum (OAM) is less satisfactory.

It is well known, that the most natural definition of OAM for quarks and gluons cannot be separated in a gauge invariant way from the corresponding spin terms⁴. However, recently, new definitions of angular momentum have been implemented to accommodate gauge invariance^{5,6}, and from them adequate twist two OAM distributions have been constructed.

In this respect, three different possibilities have been investigated. One proceeds by choosing a particular gauge^{4,7,8}. The OAM operator leads to the naive definition of orbital angular momentum up to effects not controlled by the gauge fixing. A second, maintains gauge invariance, by loosing covariance, defining the distributions only in the class of reference frame where the nucleon has a definite polarization⁹. In this case the resulting distributions can be related to the forward limit of off-forward quantities, and are measurable^{5,9,10}. The last proceeds by defining OAM operators such that the distributions are gauge invariant⁶. Furthermore, in the light-cone gauge, they reduce to

the natural definitions⁴. At present, however, no physical process has been proposed to access them.

Evolution equations for the OAM distributions have been derived^{7,8,9,11,12}, and they have been numerically solved by using as input data-inspired OAM distributions¹³.

During the last few years we have developed a scheme to study distributions based on model calculations¹⁴. This procedure has been worked out thus far to leading order in the twist expansion and therefore we should compare with the data only at high Q^2 , where the contribution from the non leading twists vanishes. In this talk we present the OAM distributions obtained by evolving those, properly calculated within relativistic and non relativistic models, to the experimental scale¹⁵.

2 The theoretical framework

It has been suggested in the past that the OAM contribution to the nucleon spin can be large at low^{16,17}, as well as large¹, energy scales. Since the quark spin, $\Delta\Sigma(Q^2)$, and the gluon spin, $\Delta g(Q^2)$, are observables, one may use the Spin Sum Rule⁴ for the nucleon,

$$\frac{1}{2}\Delta\Sigma(Q^2) + \Delta g(Q^2) + L_q(Q^2) + L_g(Q^2) = \frac{1}{2} \quad (1)$$

to determine the global OAM contribution to the spin. The problem of separating the OAM in the quark and gluon fractions in a gauge invariant way, already addressed in⁴, is a cumbersome one.

We will adopt here the gauge independent, twist-2, new definition for the quark OAM distribution, given in ref.⁹. This definition mixes the polarized and unpolarized singlet quark distributions with the forward limit of off-forward parton distributions (OFFPD). Since the OAM matrix element is not a Lorentz scalar, there is an ambiguity in this definition for any relativistic quantum theory. To avoid it, one must take for QCD a system of coordinates where the nucleon has a definite helicity, thus loosing covariance.

We proceed to use this last theoretical development, to perform a phenomenological model analysis of the OAM distributions, using relativistic as well as non-relativistic quark models.

Let us first discuss the definition of the OAM for a relativistic model. According to Ref.⁹, if we assume that the nucleon is moving in the z direction and is polarized with helicity $+1/2$, the quark OAM distribution is given by,

$$L_q(x, Q^2) = \frac{1}{2} [x(\Sigma(x, Q^2) + E_q(x, Q^2)) - \Delta\Sigma(x, Q^2)] , \quad (2)$$

where $\Sigma(x, Q^2)$ ($\Delta\Sigma(x, Q^2)$) is the usual unpolarized (polarized) *singlet* quark distribution and $E_q(x, Q^2)$ is the *forward limit* of the helicity-flip, chiral odd, twist-two OFFPD $E(x, \Delta^2, \Delta \cdot n)$ ⁵. The latter quantity is defined through the twist-2 part in the the following twist expansion

$$\begin{aligned} \int \frac{d\lambda}{2\pi} \langle P' | \bar{\psi}(-\lambda n/2) \gamma^\mu \psi(\lambda n/2) | P \rangle &= H(x, \Delta^2, \Delta \cdot n) \bar{U}(P') \gamma^\mu U(P) \\ &+ E(x, \Delta^2, \Delta \cdot n) \bar{U}(P') \frac{i\sigma^{\mu\nu} \Delta_\nu}{2M} U(P) + \dots, \end{aligned} \quad (3)$$

where $P(P')$ is the 4-momentum of the initial (final) nucleon in a virtual Compton scattering process, $\Delta_\mu = P'_\mu - P_\mu$, $n = (1, 0, 0, -1)/2\Lambda$, Λ is fixed by the choice of the reference frame, and $H(x, \Delta^2, \Delta \cdot n)$ is the helicity-conserving, chiral even, twist-2 OFFPD whose forward limit is the usual forward unpolarized parton distribution. In the definitions above, the forward limit corresponds to $\Delta^2 \rightarrow 0$, $\Delta \cdot n \rightarrow 0$.

In the non-relativistic case, the nucleon wave function is given in general by an expansion in terms of the eigenstates of some approximate hamiltonian. Let N label the quantum numbers of the eigenstates, i.e., principal quantum number, orbital angular momentum, spin, ..., then

$$\Psi(\vec{p}_1, \vec{p}_2, \vec{p}_3) = \sum_N a_N \psi_N(\vec{p}_1, \vec{p}_2, \vec{p}_3) \quad (4)$$

The OAM quark parton distribution, generalizing our approach developed for unpolarized and polarized distributions ¹⁴, is determined by ¹⁵

$$L_q(x, Q^2) = 2\pi M \sum_N |a_N|^2 \int_{|p_-(x)|}^{\infty} dp p L_{q,N}^z(p) , \quad (5)$$

where

$$L_{q,N}^z(p) = \langle \psi_N(\vec{p}_1, \vec{p}_2, \vec{p}_3) | \sum_{i=1}^3 L_i^z \delta(\vec{p} - \vec{p}_i) | \psi_N(\vec{p}_1, \vec{p}_2, \vec{p}_3) \rangle, \quad (6)$$

and the lower integration limit is fixed by energy conservation ¹⁴.

Having set down the framework which defines the OAM distributions at the hadronic scale, we proceed to calculate them explicitly in two models and to study their evolution.

3 OAM parton distributions at high Q^2

We proceed to study the OAM distribution in two different scenarios for proton structure: i) a non-relativistic scheme based on the Isgur-Karl model¹⁸; ii) a relativistic approach, as described by the MIT bag model¹⁹.

For the non-relativistic scenario we consider initially the Isgur-Karl model with a proton wave function given by a harmonic oscillator potential including contributions up to the $2\hbar\omega$ shell²⁰. In this case the wave function, Eq. (4), is given by

$$|N\rangle = a_S|^2S_{1/2}\rangle_S + a_{S'}|^2S'_{1/2}\rangle_S + a_M|^2S_{1/2}\rangle_M + a_D|^4D_{1/2}\rangle_M, \quad (7)$$

where we have used the spectroscopic notation $|^{2S+1}X_J\rangle_t$, with $t = A, M, S$ being the symmetry type. The coefficients were determined by spectroscopic properties to be: $a_S = 0.931$, $a_{S'} = -0.274$, $a_M = -0.233$, $a_D = -0.067$.

Calculating Eq. (6) using the wave function Eq. (7), one gets for the parton distribution, Eq. (5)¹⁵,

$$L_q(x, \mu_0^2) = |a_D|^2 \frac{M}{\alpha\sqrt{\pi}} \left(\frac{3}{2}\right)^{3/2} \left(\frac{1}{5} \frac{p_-^4}{\alpha^4} + \frac{13}{30} \frac{p_-^2}{\alpha^2} + \frac{23}{45}\right) e^{-\frac{3p_-^2}{2\alpha^2}}, \quad (8)$$

where α^2 is a parameter of the model. Note that only the small $|^4D_{1/2}\rangle_M$ wave component gives a contribution to the distribution.

In the relativistic scenario, we evaluate the twist-two distribution Eq. (2) in the MIT bag model. The term $\Delta\Sigma(x, \mu_0^2)$ in Eq. (2) is discussed for the bag in ref.²³. To calculate Eq.(2) we need the quantity $\Sigma(x, \mu_0^2) + E_q(x, \mu_0^2)$, which is given by the forward limit of the OFFPD distribution $H(x, \Delta^2, \Delta \cdot n) + E(x, \Delta^2, \Delta \cdot n)$. The result for the latter in the bag, calculated by using the general definition (Eq. (3)), is to be found in Eq.(29) of ref.²¹, from which we have obtained the forward limit. The explicit expression for such a limit can be found in Ref.¹⁵.

In both cases, Isgur-Karl (IK) and MIT, we use the corresponding support correction as defined in¹⁴ and²², respectively.

Once the distributions $L_q(x, \mu_0^2)$ have been obtained at the low (hadronic) scale of the model, we perform a LO QCD evolution according to the equations displayed in refs.^{8,9,11,12,13}. These contain a complicate mixing between

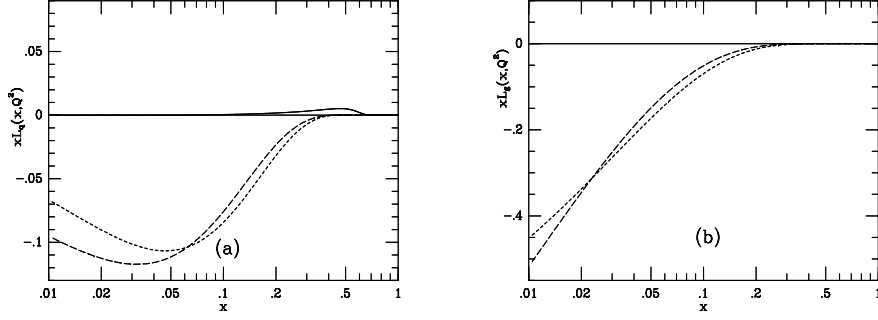


Figure 1. Proton OAM distributions in the IK model for the quarks, (a), and for the gluons, (b). The full curves show the initial distributions at the hadronic scale of $\mu_0^2 = 0.08 \text{ GeV}^2$, where a negligible fraction of the nucleon momentum is carried by the gluons; the dashed curves represent the LO-evolved distributions at $Q^2 = 10 \text{ GeV}^2$; the long-dashed curves give the LO-evolved distributions at $Q^2 = 1000 \text{ GeV}^2$.

$L_{q(g)}(x, \mu_0^2)$, $\Delta\Sigma(x, \mu_0^2)$ and $\Delta g(x, \mu_0^2)$, a feature which will be very relevant in the analysis of the data.

The results of our analysis are shown in Figs. 1 through 5. In Fig. 1 we show the IK result for quarks (gluons) in (a) ((b)); The full curve corresponds to the initial distribution, which is missing in (b), since we start from a very low hadronic scale where no valence gluons exist. At LO the hadronic scale corresponds to $\mu_0^2 \simeq 0.08 \text{ GeV}^2$. The dashed curves correspond to the result of the evolution from the hadronic OAM distributions, to $Q^2 = 10 \text{ GeV}^2$ (short-dashed) and to $Q^2 = 1000 \text{ GeV}^2$ (long-dashed).

We can summarize the results of the calculation as follows: i) the evolved distributions are negative; ii) the magnitude of the distributions increases with Q^2 at low x ; iii) the magnitude of $L_q(x, Q^2)$ is *small* but increases with respect to the tiny starting distribution (Eq. (8)); iv) though gluons are assumed to be negligible at the hadronic scale, $L_g(x, Q^2)$ becomes much larger than $L_q(x, Q^2)$ at high Q^2 . We show in Fig. 2 the same analysis for the MIT bag model. Here the initial L_q is much larger, but the result of the evolution is qualitatively basically the same.

Thus our first conclusion is that there is little model dependence for different initial OAM distributions. In this case their structure does not seem to influence very much the evolution. It is clear that the other inputs of the equations, $\Delta\Sigma(x, \mu_0^2)$ and $\Delta g(x, \mu_0^2)$, are the dominating features.

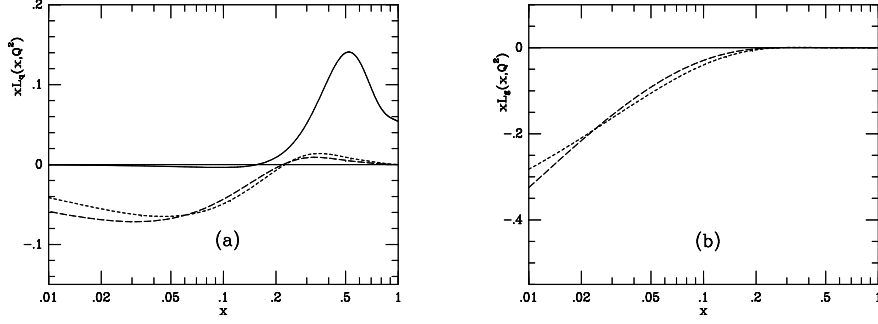


Figure 2. The same as in Fig.1, but for the MIT model. It should be noticed that the distribution at the hadronic scale of $\mu_0^2 = 0.08 \text{ GeV}^2$ is shown as it comes out from the model calculation, before the support correction is implemented. For this reason it does not go to zero at $x = 1$.

For these results the initial scale has been very low and therefore no initial gluon distribution was required. In Fig. 3 we show the result of the evolution for the IK model starting from a higher scale, $\mu_0^2 \simeq 0.23 \text{ GeV}^2$. At this hadronic scale, for LO, about 40 % of the proton momentum must be carried by the gluons. The polarized gluon contribution is built starting from the valence quark distributions as done in ¹⁴ and suggested in ²⁴, and we define $L_g(x, \mu_0^2)$ from $L_q(x, \mu_0^2)$ using the same prescription.

Again the same features as in the first analysis are found. Recapitulating, our results show that the input distributions $L_q(x, \mu_0^2)$ and $L_g(x, \mu_0^2)$ do not seem to determine the behavior of their evolved ones, which turns out to be governed by the singlet polarized distributions $\Delta g(x, \mu_0^2)$ and $\Delta \Sigma(x, \mu_0^2)$, due to their mixing in the evolution equations. To check to what extent such a statement, stressed also in ¹³, is valid, we analyze in Fig. 4 the results of a modification of the IK model, the so called D model, already studied in ²⁵. In this variant model, the D wave probability is set large to reproduce the axial coupling constant of the nucleon ¹⁶. This condition requires the following choice of the parameters in Eq. (7): $a_S = 0.894$, $a_{S'} = 0$, $a_M = 0$, $a_D = -0.447$, i.e., the probability to find a nucleon in the D wave is about 20 %. Moreover we have introduced also in the D Model scenario polarized valence gluons, as we did for the IK scenario of Fig.3. From the figure it is clear that, while the result for the gluons does not differ in a relevant way from the ones found before with the various models, the result for

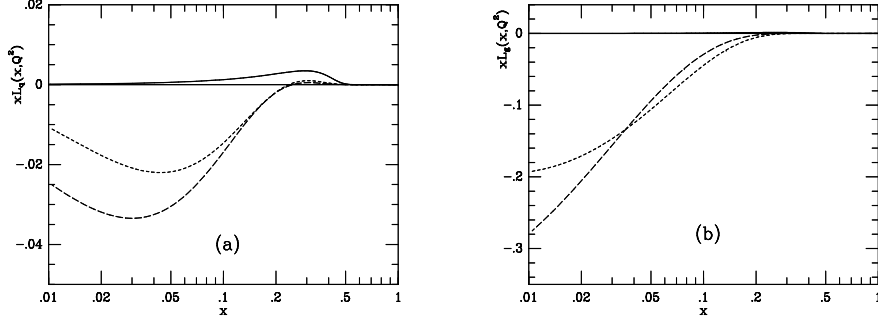


Figure 3. Proton OAM distributions in a modified IK model (see text) for the quarks, (a), and the gluons, (b). The full curves show the initial distributions at the hadronic scale of $\mu_0^2 = 0.23 \text{ GeV}^2$, where around 40 % of the nucleon momentum is carried by the gluons; the dashed curves represent the LO-evolved distributions at $Q^2 = 10 \text{ GeV}^2$; the long-dashed curves give the LO-evolved distributions at $Q^2 = 1000 \text{ GeV}^2$. The initial gluon distribution is so small, in relation with the final one, that it does not show up in (b).

$L_q(x, Q^2)$ does, this distribution becoming rather large and positive for large x . It is important to stress that in order for this to occur two mechanisms were needed, a large initial OAM distribution (as in the MIT bag Model), and a higher hadronic scale (as provided by the valence gluons). As shown previously, the independent action of the two mechanisms does not lead to this behavior. Thus, $\Delta g(x, \mu_0^2)$ and $\Delta \Sigma(x, \mu_0^2)$ are governing the evolution as long as they are much larger than $L_q(x, \mu_0^2)$ at the initial scale. When they have similar size the above statement is not true any more. Note that the IK interaction together with the choice of parameters of the D model does not describe the hadron spectrum. Nonetheless, other models of interaction (for example ^{16,17}) predict at the low scale a large OAM and fit the spectrum. We conclude therefore that a precise knowledge of the OAM distributions will serve to distinguish among the models. In Fig. 5 we show the evolution of the various contributions to the spin sum rule, Eq. (1). Fig. 5 (a) corresponds to the modified IK scenario used in Fig. 3, where at the scale of the model the OAM carried by quarks and gluons is very small and the rest of the proton spin is almost equally shared between quarks and gluons spins ($L_q(\mu_0^2) + L_g(\mu_0^2) \simeq 0.01$, $\Delta \Sigma(\mu_0^2) \simeq 0.48$ and $\Delta g(\mu_0^2) \simeq 0.25$), whereas Fig. 5 (b) corresponds to the extreme scenario used already in Fig 4, the so called D model, with a large initial OAM ($L_q(\mu_0^2) = 0.145$, $L_g(\mu_0^2) = 0.055$, $\Delta \Sigma(\mu_0^2) \simeq 0.4$ and

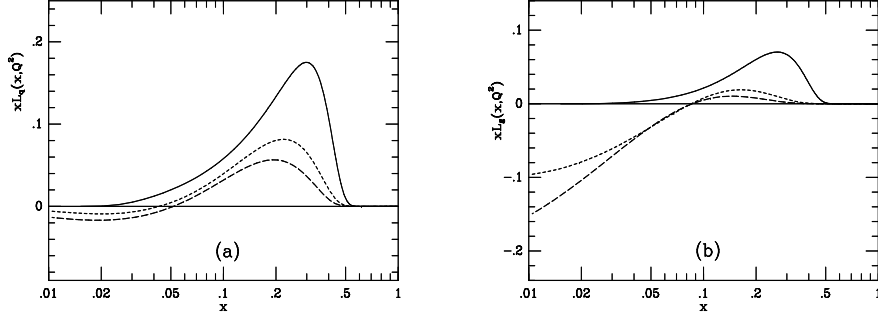


Figure 4. Proton OAM distributions for the “D-Model” (see text), for the quarks, (a), and the gluons, (b). The full curves show the initial distributions at the hadronic scale of $\mu_0^2 = 0.23 \text{ GeV}^2$, where around 40 % of the nucleon momentum is carried by the gluons; the dashed curves represent the LO-evolved distributions at $Q^2 = 10 \text{ GeV}^2$; the long-dashed curves give the LO-evolved distributions at $Q^2 = 1000 \text{ GeV}^2$.

$\Delta g(\mu_0^2) \simeq 0.1$). As predicted by total angular momentum conservation¹ and already obtained in¹³ as a model-independent feature of the evolution equation, it is seen that at large Q^2 the huge negative contribution $L_g(Q^2)$ basically cancels out with the positive $\Delta g(Q^2)$. Anyway, the role of the quark OAM is found to be very important in the second scenario (cf. Fig. 5(b)), being at large Q^2 the largest contribution to the saturation of the spin sum rule. Again, we see that quark OAM, due to evolution, can be important at large Q^2 if it is not negligible at the scale of the model, whereas the gluons OAM, though it is large, is basically cancelled by the gluons spin.

4 Conclusions

We have studied the OAM distributions as defined newly in order to take into account gauge invariance.

We have seen that evolution, as in previous calculations¹⁴, plays a major role in the outcome of the predictions. The fact that the gluon and quark spin singlet distributions mix in these equations with the quark OAM distributions, implies that for large Q^2 large contributions from the OAM are to be expected, even if they are not present at the hadronic scale. Thus, two scenarios arise in a natural way. One, the more conventional one, as described by the more traditional models, is defined by quark OAM distributions at a

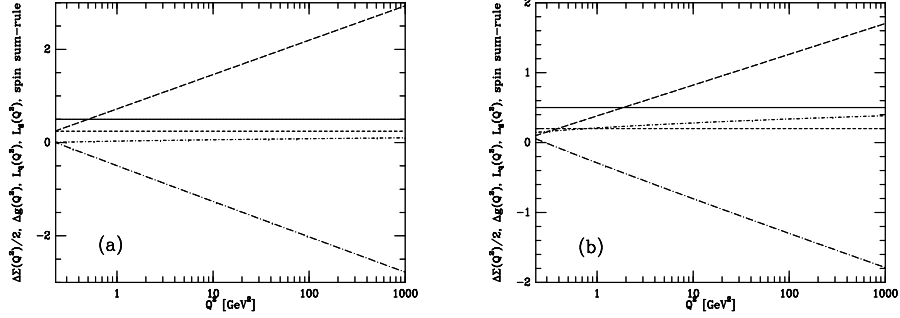


Figure 5. The contributions to the proton spin sum rule, Eq. (1), according to: (a) the modified IK scenario of Fig. 3; (b) the “D model” scenario of Fig. 4. The dashed curve shows $\frac{1}{2}\Delta\Sigma(Q^2)$, the long-dashed one $\Delta g(Q^2)$, the dot-dashed curve is $L_q(Q^2)$, the dot-long-dashed curve gives $L_g(Q^2)$ and the full curve represents the sum of the previous four terms, giving the spin sum rule ($J = \frac{1}{2}$).

small hadronic scale. In this scenario the evolved distributions are large, negative and almost model independent and angular momentum DIS physics is dominated by the quark and gluon spin singlet distributions, not by OAM distributions at the hadronic scale. A second scenario is defined by quark and gluon OAM distributions at a higher hadronic scale. In the latter, soft evolution scenario, the initial distributions are important and therefore DIS physics may be able to discriminate between models. If the OAM distributions are large the outcome of the evolution is strongly dependent on the initial distributions and completely different from that of the first scenario.

Finally the gluon OAM distributions become huge through evolution, even if they are not present at the hadronic scale. However, as it is well known¹, the gluon OAM and gluon spin contributions cancel to a great extent in the nucleon spin, but not so in other moments. Our past experience suggests that LO results provide a reasonable *qualitative* approximation and we do not expect that NLO corrections can spoil their general features.

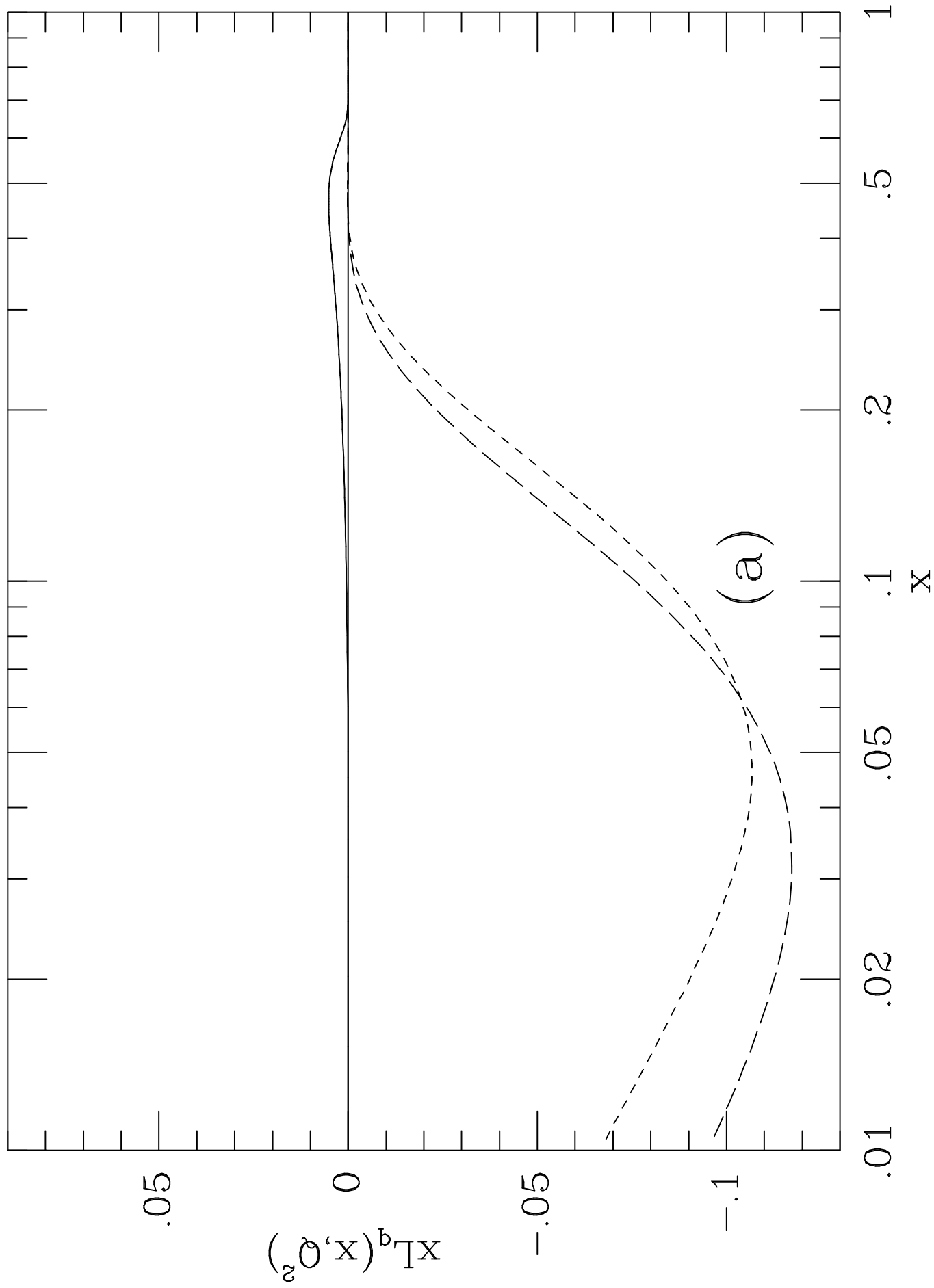
Many phenomenological implications have arisen of our study. A careful analysis of gauge invariance^{5,6,9} has permitted us to obtain many observables, which may not only lead to a better understanding of the proton spin, but to describe the proper behavior of QCD at low energies, i.e., in the confining region. These observations are instrumental in defining the picture of the proton that should be used for describing low energy properties.

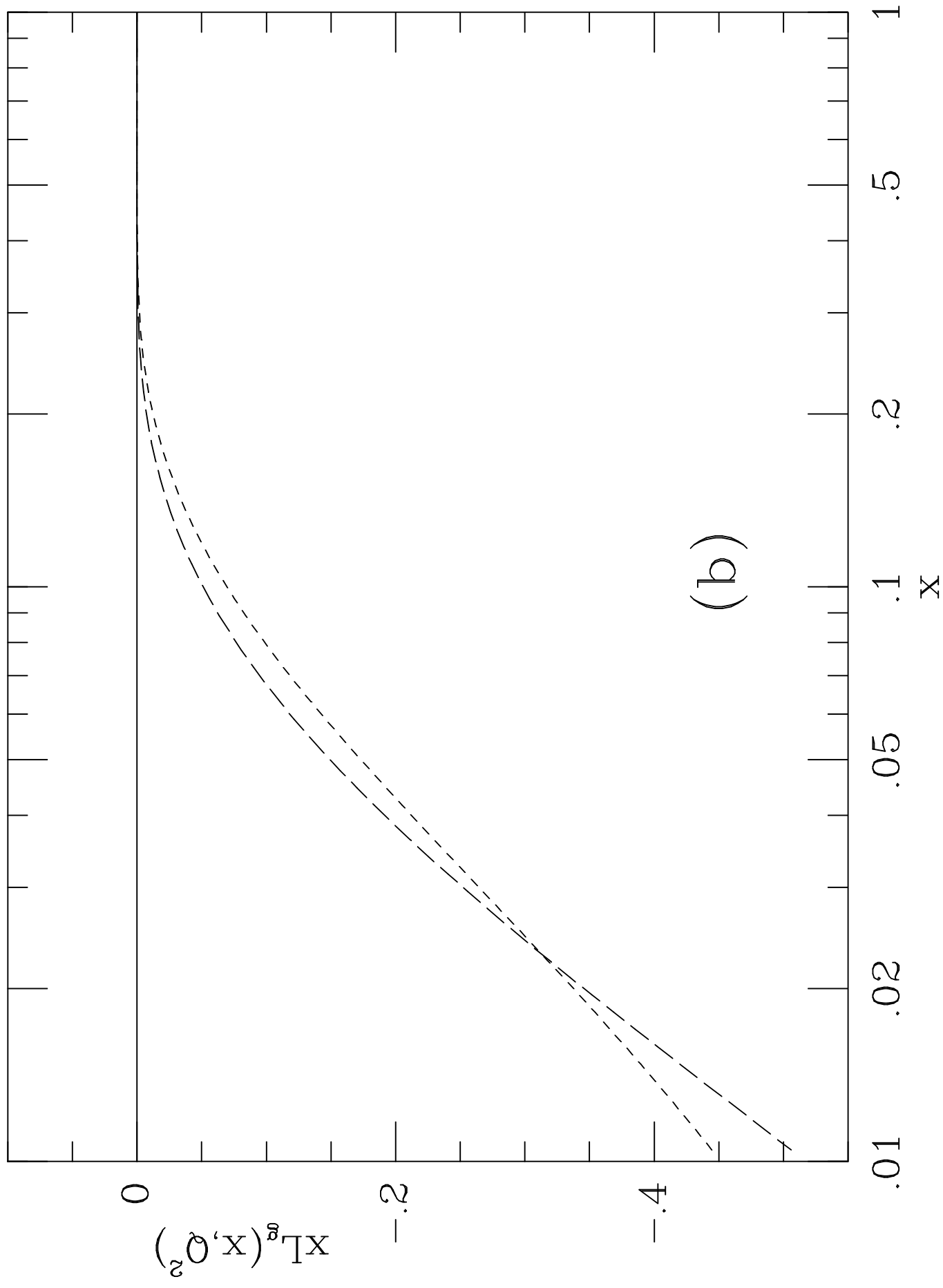
Acknowledgments

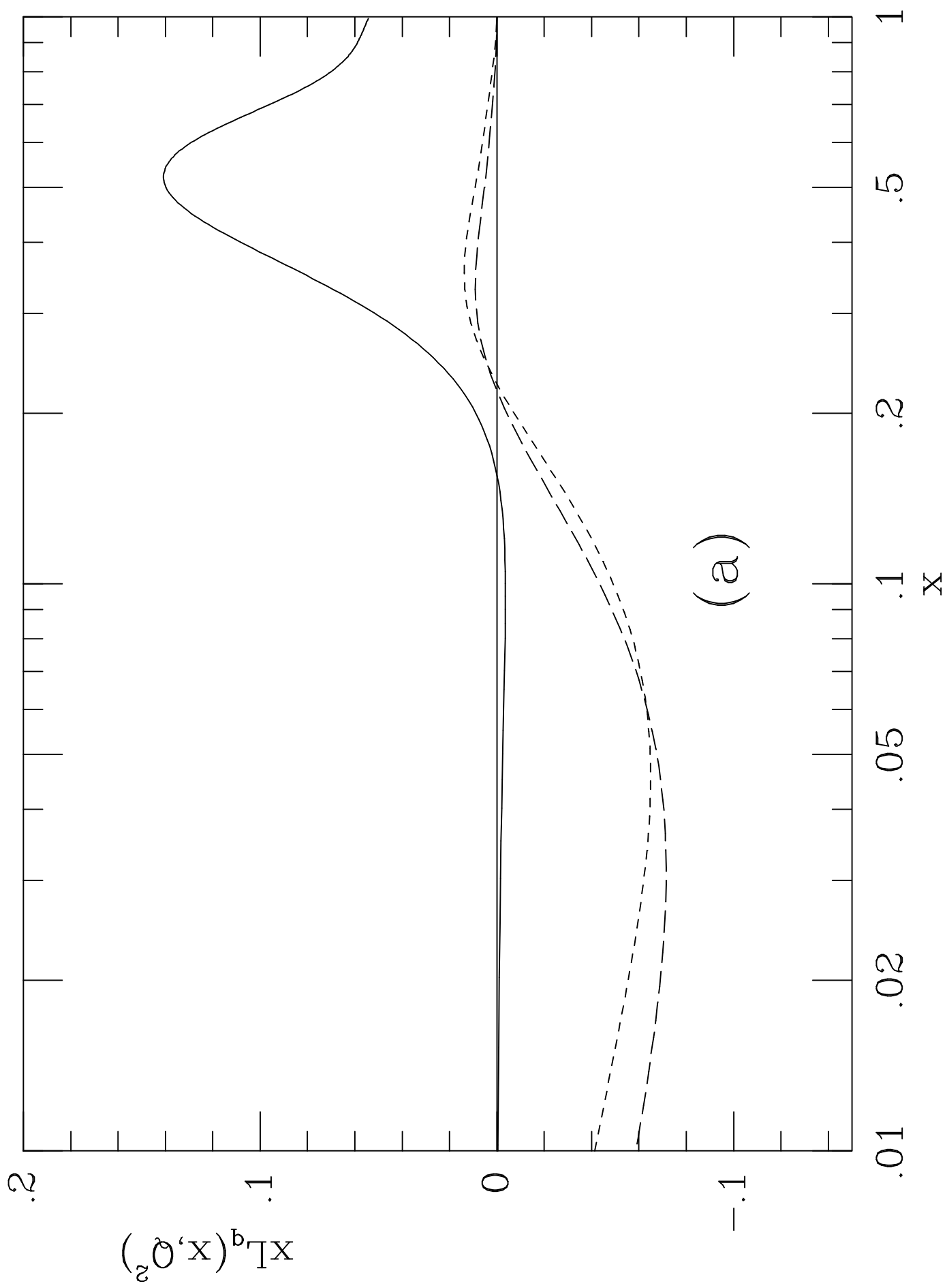
S.S. thanks the organizers for the invitation. Supported in part by DGICYT-PB97-1227 and TMR programme of the European Commission ERB FMRX-CT96-008.

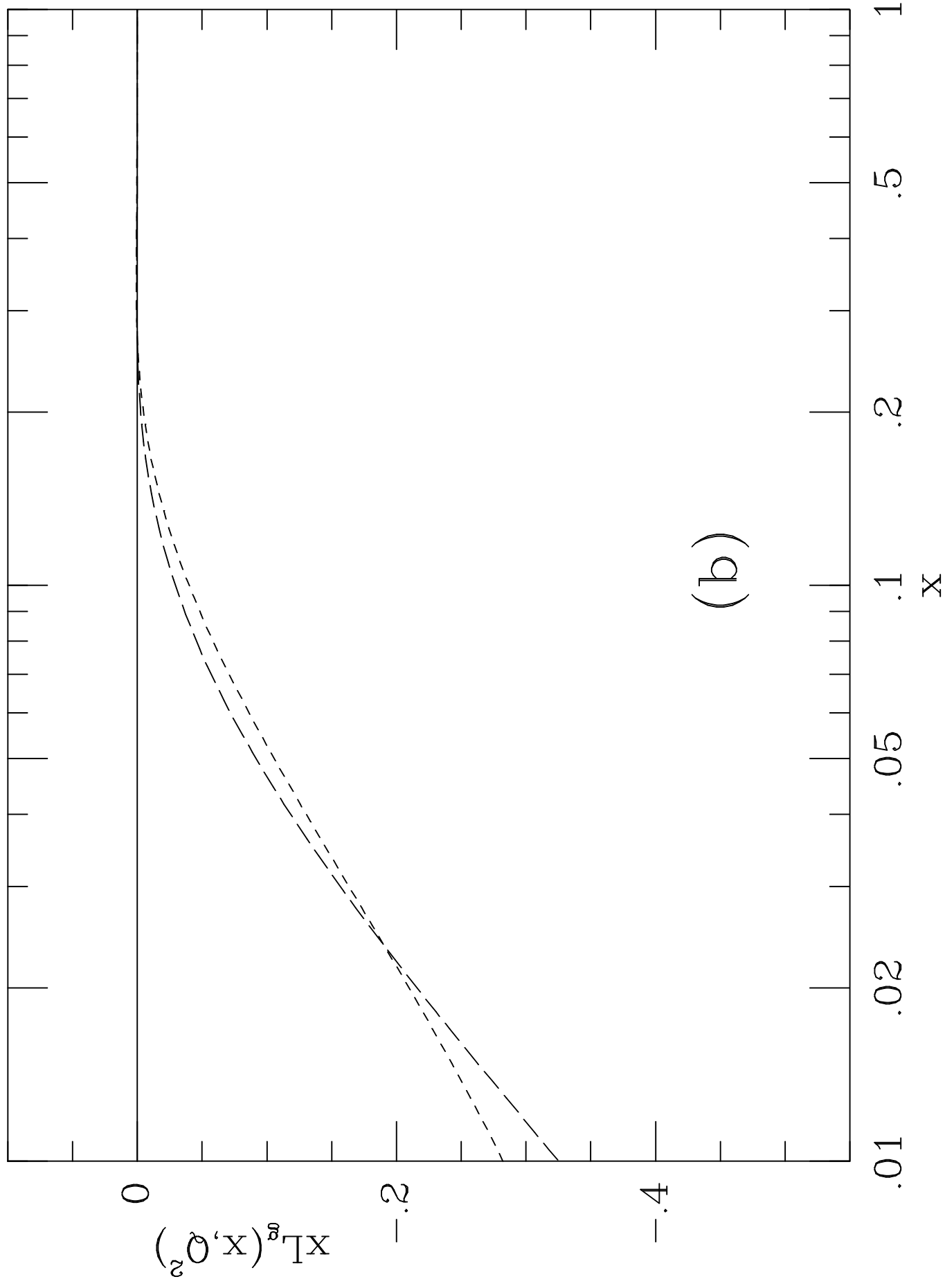
References

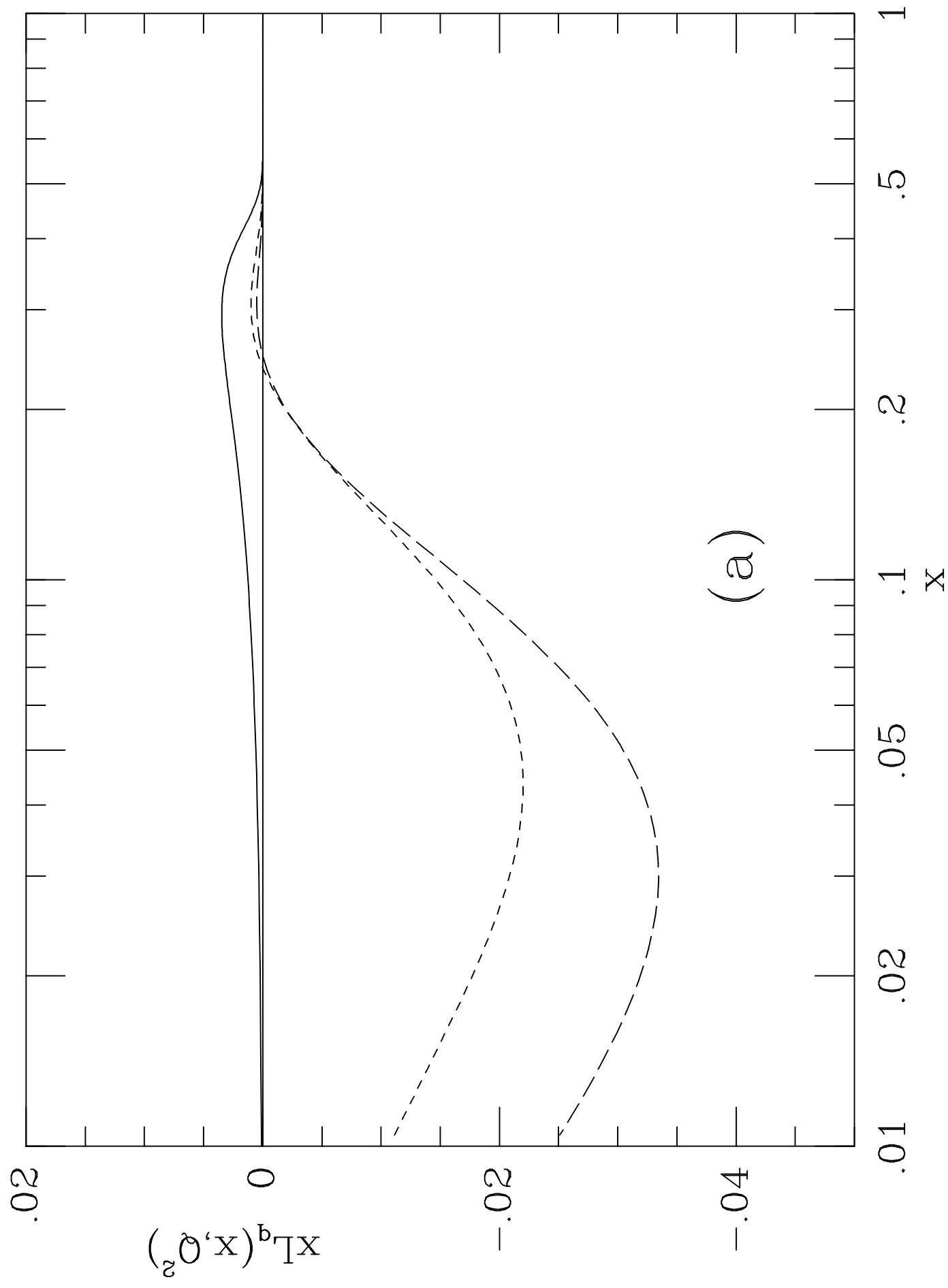
1. P.G. Ratcliffe, Phys. Lett. B 192 (1987) 180.
2. P.K.A. de Witt Huberts, this Conference.
3. A. Drago, this Conference.
4. R. L. Jaffe and A. Manohar, Nucl. Phys. B 337 (1990) 509.
5. X. Ji, Phys. Rev. Lett. 78 (1997) 610.
6. S.V. Bashinsky and R.L. Jaffe, Nucl. Phys. B 536 (1998) 303.
7. X. Ji, J. Tang and P. Hoodbhoy, Phys. Rev. Lett. 76 (1996) 740.
8. P. Hägler and A. Schäfer, Phys. Lett. B 430 (1998) 179.
9. P. Hoodbhoy, X. Ji and W. Lu, Phys. Rev. D 59 (1999) 014013.
10. P. Hoodbhoy, X. Ji and W. Lu, Phys. Rev. D 59 (1999) 074010.
11. A. Harindranath and R. Kundu, Phys. Rev. D 59 (1999) 116013.
12. O.E. Teryaev, hep-ph/9803403.
13. O. Martin, Hägler and A. Schäfer, Phys. Lett. B 448 (1999) 99.
14. M. Traini, V. Vento, A. Mair and A. Zambarda, Nucl. Phys. A 614 (1997) 472 and references therein; S. Scopetta and V. Vento, Phys. Lett. B 424 (1998) 25.
15. S. Scopetta and V. Vento, hep-ph/9901324, Phys. Lett. B (1999) to appear.
16. V. Vento, G. Baym and A.D. Jackson, Phys. Lett. B 102 (1981) 97; V. Vento and J. Navarro, Phys. Lett. B 140 (1984) 6; *ibid* 141 (1984) 285; Nucl. Phys. A 440 (1985) 617.
17. L. M. Sehgal, Phys. Rev. D 10 (1974) 1663.
18. N. Isgur and G. Karl, Phys. Rev. D 18 (1978) 4187, D 19 (1979) 2653, D 23 (1981) 817(E).
19. T. DeGrand, R.L. Jaffe, K. Johnson and J. Kiskis, Phys. Rev. D 12 (1975) 2060.
20. M.M. Giannini, Rep. Prog. Phys. 54 (1991) 453.
21. X. Ji, W. Melnitchouk and X. Song, Phys. Rev. D 56 (1997) 5511.
22. R.L. Jaffe and G.G. Ross, Phys. Lett. B 398 (1980) 313.
23. R.L. Jaffe and X.Ji, Phys. Rev. D 43 (1991) 724.
24. M. Glück, E. Reya, A. Vogt, Z. Phys. C 48, 471 (1990).
25. M. Ropele, M. Traini and V. Vento, Nucl. Phys. A 584 (1995) 634.











(a)

